

Urban Snowpack ClNO_2 Production and Fate: A One-Dimensional Modeling Study

Siyuan Wang, Stephen M. McNamara, Katheryn R. Kolesar, Nathaniel W. May, Jose D. Fuentes, Ryan D. Cook, Matthew J. Gunsch, Claire N. Mattson, Rebecca S. Hornbrook, Eric C. Apel, and Kerri A. Pratt*



Cite This: <https://dx.doi.org/10.1021/acsearthspacechem.0c00116>



Read Online

ACCESS |

Metrics & More

Article Recommendations

Supporting Information

ABSTRACT: Nitryl chloride (ClNO_2) is formed in urban areas from the multiphase reaction of dinitrogen pentoxide (N_2O_5) on chloride-containing surfaces. ClNO_2 undergoes photolysis to produce atomic chlorine (Cl^{\bullet}), a strong atmospheric oxidant. While previous ClNO_2 studies have focused on atmospheric particulate chloride, the saline snowpack in locations impacted by sea spray and road salt usage represents an additional, potentially large, source of ClNO_2 . Here, we present the first modeling study to explore the production of ClNO_2 from the inland urban snowpack. The coupled snowpack-atmospheric one-dimensional model is constrained to and evaluated by an array of ambient measurements in Ann Arbor, Michigan, during February 2016. The model predicts strong N_2O_5 deposition onto the snowpack, with ClNO_2 formation and release to the atmosphere at low temperatures ($<\sim 260$ K). However, at higher temperatures ($>\sim 270$ K), the ClNO_2 yield is low (e.g., 10%), with ClNO_2 undergoing hydrolysis on the snow grains, making the snowpack a net sink for ClNO_2 . These results motivate measurements to quantify ClNO_2 production from the urban snowpack because of potential broader impacts on atmospheric composition and air quality.

KEYWORDS: atmospheric chemistry, snow, 1-D modeling, road salt, air quality, winter, ClNO_2 , N_2O_5



1. INTRODUCTION

Nitryl chloride (ClNO_2) is an important precursor for atomic chlorine (Cl) in the lower troposphere^{1,2} that has been observed in coastal, marine, and inland environments.³ Cl atoms can destroy the greenhouse gas methane³ and react with volatile organic compounds much faster than the hydroxyl radical, leading to an enhanced formation of ozone.^{4,5} ClNO_2 can be formed from the multiphase reaction of N_2O_5 with chloride-containing particles.⁶ Wintertime conditions of low temperatures and longer nights are particularly conducive for ClNO_2 formation.^{5,7} This is due, in part, to the slower N_2O_5 thermal dissociation at lower temperatures⁸ and reduced photolysis with less sunlight, in addition to increased particulate chloride during winter.⁹

Previous studies have focused on ClNO_2 production from ambient particles.³ However, at lower temperatures, laboratory studies have revealed efficient N_2O_5 uptake and subsequent ClNO_2 production on chloride-containing droplets (down to 262 K)¹⁰ and chloride-doped ice surfaces (220–255 K).¹¹ Therefore, it appears plausible that N_2O_5 uptake and ClNO_2 production may occur on the natural snowpack, providing yet another source for ClNO_2 in the ambient environment. This mechanism may be particularly relevant in snow-covered coastal regions influenced by sea spray aerosols, as well as in mid-latitude urban areas where chloride-containing salts and brines are widely used as de-icing agents during winter.^{9,12}

Trace gas exchange between the snowpack and ambient air involves multiple chemical and physical processes,¹³ including chemical production and removal within the snowpack, as well as physical transport such as wind pumping¹⁴ and molecular diffusion.¹⁵ The snowpack is highly porous, containing a wide range of “impurities” such as chloride, nitrate, and so forth, and from which multiphase reactions can affect the photochemistry in the overlying air,^{13,16} including in the wintertime urban environment.^{17–20} Snowpack emissions of a variety of compounds have been observed from the natural snowpack in the polar and mid-latitude regions: nitrogen oxides (NO_x),^{18,21–23} nitrous acid (HONO),^{17,22} formaldehyde (HCHO),²⁴ and molecular halogens (Cl_2 , BrCl , Br_2 , and I_2),^{25–27} for example. The snowpack also serves as a depositional sink for species such as ozone (O_3),^{28,29} N_2O_5 ,^{20,30} and nitric acid (HNO_3).²² McNamara et al.³¹ reported elevated ClNO_2 in the coastal Arctic and hypothesized multiphase reactions of N_2O_5 on the surface snowpacks, in addition to on aerosols. However, few studies have

Received: May 2, 2020

Revised: June 23, 2020

Accepted: June 24, 2020

Published: June 24, 2020

examined air–snow exchange and the chemical reactions associated with the urban mid-latitude snowpack.

The multiphase chemistry of ClNO_2 has received less attention compared to N_2O_5 and other surface-reactive species, partially due to its weaker surface reactivity. Behnke et al.³² reported ClNO_2 reactive uptake on aqueous NaCl solutions near room temperature (291 K), with the reactive uptake coefficient of ClNO_2 ranging from 4.8×10^{-6} (for pure water) to 0.27×10^{-6} (for a 4.6 M NaCl solution). In coastal California, Kim et al.³³ reported a net downward flux of ClNO_2 over the ocean, likely due to the hydrolysis of ClNO_2 at the seawater surface, consistent with the ClNO_2 uptake experiments conducted in the laboratory.³² ClNO_2 hydrolysis produces aqueous-phase chloride and nitrate.³² The production or loss of ClNO_2 at the snowpack surface is unknown.

Previous modeling studies have explored the impacts of snowpack photochemistry on atmospheric composition.^{20,34–39} Thomas et al.^{34,35} developed a simple snowpack module and coupled it to a one-dimensional (1-D) atmospheric model, finding that snowpack photochemical processes involving nitrate and bromide can explain the atmospheric nitric oxide (NO) and bromine monoxide (BrO) observed at Summit, Greenland. Toyota et al.^{36,37} developed a conceptually similar 1-D snow-atmosphere chemistry model to explore atmospheric ozone and mercury depletion in the Arctic boundary layer. They showed that atmospheric HOBr deposits onto the surface snowpack, leading to the formation and release of Br_2 and chemically linking the snowpack and overlying atmosphere.³⁶ Despite these advances in our understanding of polar air–snow interactions, to the best of our knowledge, no previous modeling studies have examined air–snow interactions involving mid-latitude halogen chemistry. In this work, a 1-D multiphase photochemical box model with a simplified snowpack module, conceptually following previous 1-D Arctic snow-atmospheric models,^{34–37} is used to examine the fate of N_2O_5 deposition onto the saline urban snowpack. The model is constrained by ambient measurements of trace gases and aerosols made in Ann Arbor, MI during February 2016, when the urban snowpack was influenced by road salt deposition.

1.1. Model Description. The 1-D model used in this work is described by McNamara et al.⁴⁰ and based on the 0-D model described in our previous work.⁴¹ The model framework is similar to that described by Toyota et al.³⁶ and Thomas et al.,³⁴ except that the snow module used in this work consists of only one thin layer (2 cm) of snow (see Section 1.3), due to the shallower snow depth in Ann Arbor, MI, compared to the Arctic tundra. The 1-D model prognostic equations, turbulent transport, gas-phase chemistry, phase-transfer, aqueous-phase chemistry, and heterogeneous chemistry are described in detail in the Supporting Information (Sections S1–S6). This model consists of 21 log-spaced vertical layers above the surface, up to 1000 m. A schematic of the 1-D model is given in Figure S1. The formulation for turbulent transport is parameterized for mid-latitude conditions (Section S3, Figures S2–S3). The model is constrained to a number of observations of trace gases and aerosols, including N_2O_5 , O_3 , NO, and other species, measured at 12 m above the surface (Section 1.2). The model scheme for ClNO_2 production in snow resulting from the N_2O_5 deposition is described in Section 1.4. N_2O_5 uptake and ClNO_2 yield on ambient particles are described in Section S7 and Figure S4, based on the parametrization described by Bertram and Thornton,⁵⁴ using online, bulk inorganic ion

measurements of ambient $\text{PM}_{2.5}$ (particulate matter with aerodynamic diameter less than or equal to 2.5 μm) Cl^- and NO_3^- .

1.2. Case Period and Measurements. The period of 17–19 February 2016 in Ann Arbor, Michigan, was selected as the case study period, based on the work of McNamara et al.⁴⁰ This case study period experienced no drastic changes in wind speed and direction, and hence was ideal for numerical modeling. There was a thin snow cover on the ground in the evening of 17 February until the morning of 18 February. The following online ambient measurements obtained at 12 m above ground level were used to constrain the model at the same height: N_2O_5 , O_3 , NO, HCl, $\text{PM}_{2.5}$ chloride, nitrate, and total aerosol surface area. A detailed description of the meteorological and chemical data and corresponding instrumentation is given in McNamara et al.⁴⁰ In this work, the purpose of the ambient measurements is to provide realistic model conditions for the scenario of N_2O_5 uptake onto snow.

Briefly, N_2O_5 and ClNO_2 mole ratios were measured using an iodide-chemical ionization mass spectrometer (THS Instruments).^{31,40,42} NO was measured using a chemiluminescence detector,⁴³ and O_3 was measured using an ozone analyzer (model 205, 2B Technologies). Gaseous HCl mole ratios and $\text{PM}_{2.5}$ chloride and nitrate mass concentrations were measured hourly using an ambient ion monitor-ion chromatograph (AIM-IC, URG Corp.).⁴⁴ The aerosol surface area (0.015–20 μm ; time-varying) was calculated from size distributions measured using a scanning mobility particle sizer spectrometer (model 3082, TSI Inc.; mobility diameter: 15–600 nm) and an aerodynamic particle sizer (model 3321, TSI Inc.; aerodynamic diameter: 0.6–20 μm).

C_2 – C_4 hydrocarbons (ethane, propane, *i*-/n-butane), formaldehyde, acetaldehyde, and acetone in the model were constrained (held constant) by offline measurements of canister samples collected at 12 m. Electropolished, stainless steel canisters were used for whole air sampling and analyzed using a Trace Organic Gas Analyzer (TOGA)⁴⁵ for HCHO and CH_3CHO , and a gas chromatograph with a flame-ionization detector for C_2 – C_4 alkanes.^{46,47} Carbon monoxide mole ratios in the model (all layers) are initialized with observations obtained in Allen Park, Michigan (closest location with measurements available), ~44 km to the east of Ann Arbor, from the Michigan Department of Environmental Quality.⁴⁸ Methane mole ratios in the model (all layers) are initialized with observations obtained at Park Falls, Wisconsin, 673 km to the West of Ann Arbor, from the National Oceanic and Atmospheric Administration (NOAA) global monitoring network.⁴⁹ While these data are from locations that are further away than ideal, these long-lived compounds (CO and methane) are not expected to directly affect ClNO_2 chemistry and the results of our modeling study.

Snow inorganic ion composition was measured and used to calculate the snow liquid fraction, as well as N_2O_5 uptake coefficients and ClNO_2 yields on the snowpack. A total of 58 surface snow samples were collected in multiple locations near the Central Campus of the University of Michigan, Ann Arbor, from 9 February to 6 March 2016. These locations span from next to the roadside (e.g., the sidewalk near North University Avenue) to locations that were not directly influenced by the traffic (e.g., the open green space located ~170 m away from the nearest road). These snow samples were stored at 233 K until analysis. The snow samples were then thawed and immediately analyzed for a number of inorganic ions

(detection limits of chloride, sulfate, nitrate, sodium, potassium, magnesium, and calcium were 0.03, 0.06, 0.005, 0.07, 0.08, 0.03, and 0.13 μM , respectively) using ion chromatography (IC; Dionex ICS 1100 and 2100 for cations and anions, respectively).

1.3. Snowpack Parameterization. In the 1-D model, a simulated snowpack (2 cm thickness) was placed beneath the lowest atmospheric layer. The snow module is conceptually similar to that in Toyota et al.^{34,36} and was previously described by Wang and Pratt.⁴¹ Snow properties were estimated based on mid-latitude conditions. Previous studies of mid-latitude snow^{50,51} demonstrated that the grain radius in the near-surface layer (a few cm) of the snowpack ranges from 40 to 500 μm , with snow density ranging from 0.14 to 0.26 g cm^{-3} . In this work, snow grain radius (r_s) was assumed to be 500 μm , and snow density was assumed to be 0.2 g cm^{-3} . The corresponding snow-specific surface area is then calculated to be 65 $\text{cm}^2 \text{g}^{-1}$.

Laboratory studies have indicated that as the temperature of a salt solution decreases below the freezing point, pure ice will form with a liquid phase at the surface of the ice that can be enriched in inorganic ions.⁵² Based on laboratory experiments, Cho et al.⁵³ parameterized the liquid fraction of brine (f_{brine}), as a function of temperature and total solute concentration, and this has been used in Arctic snow chemistry models.^{34,36} In this work, we utilize the Cho et al.⁵³ formulation to calculate the f_{brine} using the measured salt content (sum of Na^+ and Cl^-) in the melted snow samples. Other ions are not considered in the model because Na^+ and Cl^- together accounted for 92% of the measured inorganic ion concentration in snowmelt samples.⁴⁰ The freezing point depression calculated from the snow salt content is $\ll 1$ K, and is therefore negligible. Because of the lack of measurements of snow temperature, the ambient temperature measured at 12 m (Figure 1) was used for the f_{brine} calculation. Note that f_{brine} is overestimated during Period III, as snow was still visible on the ground although the ambient air temperature was above

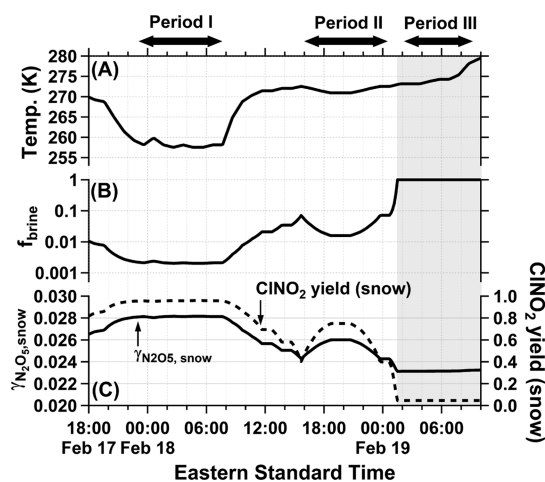


Figure 1. (A) Time series of measured ambient air temperature at 12 m above the surface, (B) calculated snow brine volume fraction (f_{brine}), and (C) calculated snowpack N_2O_5 uptake coefficients ($\gamma_{\text{N}_2\text{O}_5,\text{snow}}$) and ClNO_2 yields on snow, for 17–19 February 2016 in Ann Arbor, Michigan. Horizontal arrows indicate the three periods with different ambient temperatures, and grey shading highlights Period III, when the ambient air temperature was >273 K.

freezing (>273 K), leading to the 100% brine calculation, meaning only liquid water present.

1.4. N_2O_5 Uptake and ClNO_2 Production on Snowpack. Because the inorganic ion composition in the ambient snow samples was dominated by Na^+ and Cl^- , previous N_2O_5 uptake experiments using NaCl solutions^{10,32,54–56} are used to calculate the N_2O_5 uptake on snow grains. The effective uptake coefficient of N_2O_5 on snow ($\gamma_{\text{N}_2\text{O}_5,\text{snow,eff}}$) is given by⁵⁷

$$\frac{1}{\gamma_{\text{N}_2\text{O}_5,\text{snow,eff}}} = \frac{1}{\Gamma_{\text{diff}}} + \frac{1}{\gamma_{\text{N}_2\text{O}_5,\text{snow}}} \quad (1)$$

where $\gamma_{\text{N}_2\text{O}_5,\text{snow}}$ is the reactive uptake coefficient of N_2O_5 on snow. Γ_{diff} is a correction term for normalized gas-diffusion rate (in this case, diffusion in the snow interstitial air, SIA)⁵⁷

$$\Gamma_{\text{diff},s} = \frac{8D_{\text{SIA}}}{\bar{v}(2 \cdot r_s)} \quad (2)$$

where D_{SIA} ($\text{m}^2 \text{s}^{-1}$) is the gas diffusion coefficient in the SIA (Section S2). \bar{v} (cm s^{-1}) is the thermal speed and is given by $\bar{v} = 100 \sqrt{\frac{8RT}{\pi MW}}$, where MW is the species molecular weight (kg mol^{-1}), R is the ideal gas constant ($8.314 \text{ J K}^{-1} \text{ mol}^{-1}$), and T is the temperature (K). r_s (m) is the snow grain radius. $\gamma_{\text{N}_2\text{O}_5,\text{snow}}$ is described by the resistance analogue model (eq 3)⁵⁷

$$\frac{1}{\gamma} = \frac{1}{\alpha} + \frac{\bar{v}}{4HRT \sqrt{k^1 D_{\text{aq}}}} \quad (3)$$

where α is the dimensionless mass accommodation coefficient and H is the Henry's law constant of N_2O_5 (5 M atm^{-1}).⁵⁸ k^1 (s^{-1}) is the pseudo-first order rate in the aqueous-phase and D_{aq} ($\text{m}^2 \text{s}^{-1}$) is the aqueous diffusion coefficient ($10^{-5} \text{ cm}^2 \text{s}^{-1}$).⁴⁸ The total pseudo-first order N_2O_5 reactivity, k^1 , is given by

$$k^1 = k_{\text{H}_2\text{O}}[\text{H}_2\text{O}] + k_{\text{Cl}^-}[\text{Cl}^-] \quad (4)$$

$[\text{H}_2\text{O}]$ is the liquid water content of snow brine ($\approx 55 \text{ M} = \rho / M_{\text{H}_2\text{O}}$, where $\rho \approx 1000 \text{ g L}^{-1}$ and $M_{\text{H}_2\text{O}} = 18 \text{ g mol}^{-1}$). $[\text{Cl}^-]$ (M) is the chloride concentration in the snow brine phase, which is estimated by dividing the snow melt chloride concentrations by f_{brine} . $k_{\text{H}_2\text{O}}$ and k_{Cl^-} values are estimated based on previous aqueous-phase experiments: Gaston and Thornton⁵⁵ estimated $k_{\text{H}_2\text{O}}$ and k_{Cl^-} to be $2.7\text{--}3.9 \times 10^4$ and $0.4\text{--}2.8 \times 10^7 \text{ M}^{-1} \text{ s}^{-1}$, respectively, consistent with Bertram and Thornton.⁵⁴ In this work, $k_{\text{H}_2\text{O}}$ and k_{Cl^-} are assumed to be 3.9×10^4 and $2.8 \times 10^7 \text{ M}^{-1} \text{ s}^{-1}$, respectively. From this, the yield of ClNO_2 in snow is given by⁵⁴

$$Y_{\text{ClNO}_2,\text{snow}} = \frac{k_{\text{Cl}^-}[\text{Cl}^-]}{k_{\text{H}_2\text{O}}[\text{H}_2\text{O}] + k_{\text{Cl}^-}[\text{Cl}^-]} \quad (5)$$

2. RESULTS AND DISCUSSION

2.1. Impacts of Temperature on Calculated N_2O_5 Uptake and ClNO_2 Yield on Snow. To examine the influence of ambient temperature on snowpack N_2O_5 uptake and ClNO_2 production, the 17–19 February 2016 case study was divided into three periods based on air temperature (Figure 1). Period I corresponds to 17 February 20:00 to 18 February 10:00 (all times are in EST (Eastern Standard Time)

unless otherwise noted), when the minimum ambient temperature reached 257 K with a calculated f_{brine} near 0.002. During Period II, 18 February 20:00 to 19 February 02:00, the ambient temperature decreased from 272 K to a minimum of 270 K, then rose again to 273 K (close to the snow melting point), with the calculated f_{brine} ranging from 0.016 to 1. Finally, Period III corresponds to 19 February 2:00 to 19 February 10:00, when the ambient temperature further increased to above 273 K (H_2O freezing point), resulting in a calculated f_{brine} of 1. However, it is important to note that snow was still visible on the ground (meaning $f_{\text{brine}} < 1$), illustrating the need to measure and use surface snow temperature in the future. Therefore, while the Period III model results are biased toward a higher temperature, they present an important comparison to the lower temperatures.

Despite the wide range of temperature in this case study (257–279 K), the calculated reactive uptake coefficient of N_2O_5 on snow ($\gamma_{\text{N}_2\text{O}_5, \text{snow}}$) spans a relatively narrow range, 0.023–0.028 (Figure 1). These data are consistent with N_2O_5 uptake experiments on NaCl aerosol particles showing $\gamma_{\text{N}_2\text{O}_5, \text{snow}}$ in the range of 0.02–0.04,^{10,32,56,59–61} likely due to the short reacto-diffusive length of N_2O_5 on NaCl particles (<5 nm),⁵⁵ limiting the N_2O_5 -chloride reaction to the surface. A previous study also showed that nitrate content in the condensed-phase can suppress the uptake of N_2O_5 .⁵⁴ In the present work, the surface snow nitrate content was consistently low (median: 40 μM) compared to other ions, while the chloride content was much higher (median: 234 μM) than nitrate (Figure 2). Therefore, the impact of nitrate on the N_2O_5 uptake on snow is expected to be minimal during this study.

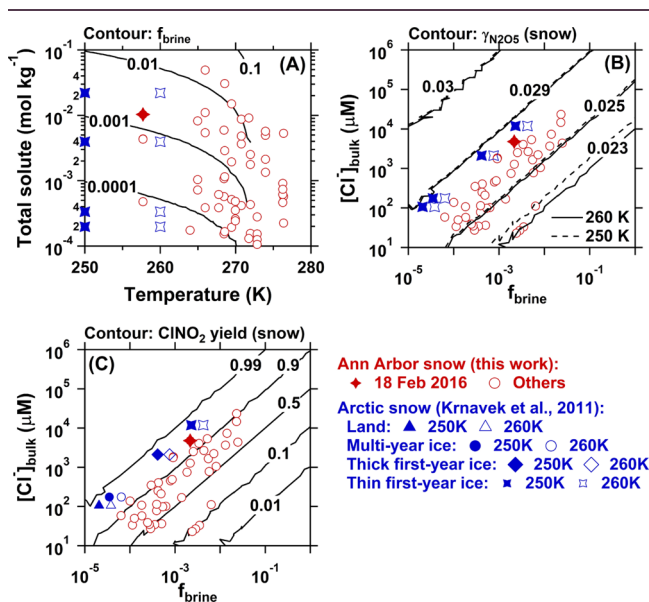


Figure 2. (A) Calculated f_{brine} as a function of total measured inorganic ion solute molality and ambient temperature. (B) Calculated $\gamma_{\text{N}_2\text{O}_5, \text{snow}}$ and (C) ClNO_2 yield on snow as a function of measured bulk snow chloride concentration and calculated f_{brine} . Red symbols show daily Ann Arbor bulk snow samples collected on 18 February (case study period) and other dates during the same study. Blue symbols represent Arctic snow measurements from Kravack et al.⁶²

The calculated snowpack ClNO_2 yield is sensitive to f_{brine} and hence to temperature. As shown in Figure 1, when ambient temperature and f_{brine} were low during Period I (~257 K and $f_{\text{brine}} \sim 0.002$, respectively), the snow ClNO_2 yield is calculated to be above 0.9, consistent with previous ClNO_2 yield measurements on halide-doped ice at 220–258 K (ClNO_2 yield near unity with high chloride/bromide ratio).¹¹ During Period II, when the ambient temperature increased (270–272 K) and f_{brine} ranged from 0.016 to 0.072, the ClNO_2 yield on snow is calculated to range from 0.5 to 0.75. Finally, during Period III, when the ambient temperature is above 273 K, the calculated f_{brine} was 1.0 (an overestimate, because snow was still present, as previously discussed), and the snow ClNO_2 yield was calculated to be only 0.05. The decreasing snow ClNO_2 yield with increasing temperature and water content (f_{brine}) is consistent with previous laboratory experiments that reported ClNO_2 yield increases with increasing chloride/ H_2O ratio.⁵⁴

Comprehensive sensitivity tests of temperature and f_{brine} on $\gamma_{\text{N}_2\text{O}_5, \text{snow}}$ and ClNO_2 yield (snow) are provided in Figure 2. Conditions of this sensitivity test (temperature: 250–280 K, salt content: 10^1 – $10^6 \mu\text{M}$) cover a wide range, from warm and salty mid-latitude snow (measured in this study) to cold and pristine snow, more relevant to remote or polar regions.⁶² As shown, f_{brine} increases with increasing temperature, but it is more sensitive to temperatures above 260 K. For temperatures below 260 K, f_{brine} is more dependent on the solute concentration. In this sensitivity test, $\gamma_{\text{N}_2\text{O}_5, \text{snow}}$ is calculated to span a fairly narrow range (0.023–0.030). In contrast, the ClNO_2 yield on snow ranges from ~0.1 to above 0.9 and is sensitive to both chloride concentration and f_{brine} (and hence temperature). In general, higher chloride concentrations lead to higher calculated ClNO_2 yields, while increasing f_{brine} lowers the ClNO_2 yield because of the higher water content competing with ClNO_2 formation (eq 4).

2.2. Modeled ClNO_2 from the Snowpack. The 1-D model reveals unique insights into the multiphase chemistry and transport of trace gases, such as NO_x , O_3 , N_2O_5 , and ClNO_2 , as well as the surface–atmosphere interactions (Figure S5 and Section S8 in the Supporting Information). In this section, we explore the potential of urban salty snowpack being a source of ambient ClNO_2 using the multiphase 1-D model, based on the estimated $\gamma_{\text{N}_2\text{O}_5, \text{snow}}$ and ClNO_2 yield in Figure 1. In addition to simulating ClNO_2 snowpack production, we include simulations of particle-phase ClNO_2 production for comparison. A number of studies have discussed the overestimation of the N_2O_5 uptake and ClNO_2 yield on particles when calculated using the bulk approach, resulting in an overestimation of ClNO_2 production.^{2,63–68} This has previously been attributed to the presence of particulate organics, nitrate, and other components.^{54,69–73} McNamara et al.⁴⁰ discussed the impacts of the aerosol mixing state (distribution of chemical components across the population of individual particles) on the simulation of ClNO_2 production on particles for the same period of measurements discussed here. In this work, our goal is to focus on the potential role of the salty urban snowpack on ambient ClNO_2 .

Three sets of model configurations are run, with the results shown in Figure 3: (a) Snow + Particles (ClNO_2 formation from both snowpack and atmospheric particles); (b) Particles only (ClNO_2 formation from atmospheric particles only); and (c) Snow only (ClNO_2 formation from snowpack only). All

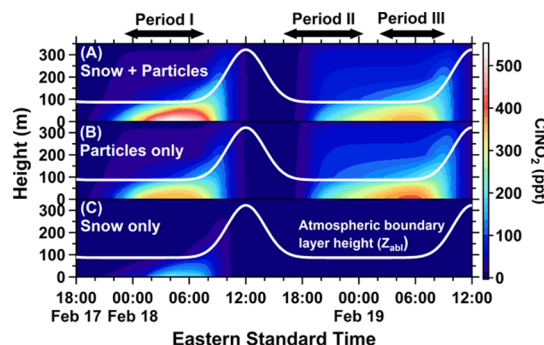


Figure 3. Modeled ClNO_2 as a function of height and time, in different scenarios: ClNO_2 production from snow + particles (A), particles only (B), and snow only (C), as well as the modeled atmospheric boundary layer height (Z_{abl}) represented by the white lines.

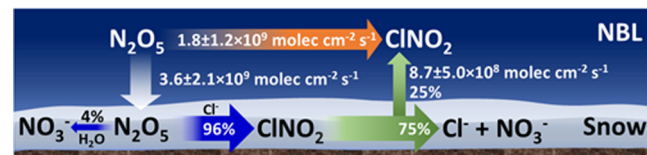
three cases predict strong ClNO_2 production within the nocturnal boundary layer (NBL) during Period I. ClNO_2 production from atmospheric particles dominates (68–100%) in the NBL, possibly due to the stable conditions in the NBL limiting N_2O_5 deposition. The snowpack contributes ~32% of ClNO_2 formation (column integral), showing the potential importance of the snowpack in urban air quality. During this period, the calculated $\gamma_{\text{N}_2\text{O}_5, \text{snow}}$ and snow ClNO_2 yield are 0.028 and 0.9, respectively, in comparison to the corresponding calculated values for particles: 0.028 ± 0.002 (average \pm standard deviation) and 0.7 ± 0.1 , respectively. In the early morning of 18 February, the boundary layer height increases from ~ 90 to ~ 300 m, leading to upward transport of ClNO_2 , which quickly photo-dissociates. During Periods II & III, however, the snow-only simulation predicts virtually no ClNO_2 from the snowpack (up to 14 ppt). Interestingly, the Snow + Particle case predicts lower ClNO_2 than the Particles only case within the NBL because the model predicts that the snowpack is a net sink of ClNO_2 under the conditions of Period III. Below, we explore the mechanisms explaining these trends.

The vertical transport of N_2O_5 and ClNO_2 depends largely on atmospheric stability. The model calculated maximum eddy diffusivity at night is $\sim 0.2 \text{ m}^2 \text{ s}^{-1}$, which is nearly two orders of magnitude lower than the calculated daytime maximum of $8.7 \text{ m}^2 \text{ s}^{-1}$ (Figure S2). As shown in Figure 3, the model predicts a strong vertical gradient of ClNO_2 within the NBL. At 02:00 h on 18 February, the Particles only case predicts that 21% of ClNO_2 remains in the lowest 20 m, with 72% in the NBL. The Snow only case, however, predicts that 76% of ClNO_2 is confined in the lowest 20 m, with 98% in the NBL. The combined case with ClNO_2 production both on snow and lofted particles predicts that 39% of ClNO_2 remains in the lowest 20 m, with 80% in the NBL. All three cases predict a certain amount of ClNO_2 produced in the residual layer (2% in the Snow only case, 28% in the Particles only case, and 20% in the Snow + Particles case). Note that in this work horizontal advection is not included in the model. Therefore, in this work, ClNO_2 in the residual layer is produced from the multiphase chemistry involving precursors (NO_x , O_3 , and particulate chloride) lofted during daytime (with 1 day spin-up), reflecting the localized influence on the residual layer. Previous studies have reported ClNO_2 production in the residual layer,^{74,75} where the chemical composition in the residual layer may be affected by advection. Because of the lack of vertically resolved

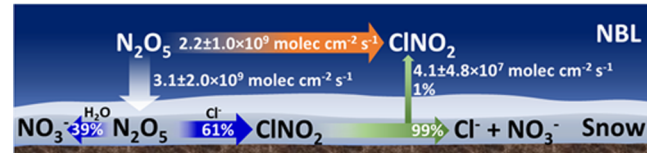
aerosol measurements, the aerosol surface area used in the model is constant vertically. The impact of the residual layer is beyond the scope of this work, as our focus is on surface production.

The modeled N_2O_5 and ClNO_2 budgets in the NBL and surface snowpack for the Snow + Particles model scenario are shown in Figure 4 for Periods I, II, and III. N_2O_5 deposition

Period I: $\sim 258 \text{ K}$



Period II: $\sim 272 \text{ K}$



Period III: $272 \rightarrow 280 \text{ K}$



Figure 4. Modeled N_2O_5 and ClNO_2 budgets in the surface snowpack and NBL during Periods I, II, and III, for the Snow + Particle model scenario. Production and removal are shown as column rates ($\text{molecules cm}^{-2} \text{ s}^{-1}$) integrated through the NBL (~ 100 m). Numbers represent average (\pm standard deviation) column rates during each period. Percentages denote the fractional contribution of each pathway to the total removal of snowpack N_2O_5 or ClNO_2 .

onto the snowpack occurs during all three periods. The modeled average downward flux of N_2O_5 ranges from 2.9×10^8 to 4.7×10^8 molecules $\text{cm}^{-2} \text{ s}^{-1}$, corresponding to a N_2O_5 deposition velocity of 0.23 – 1.9 cm s^{-1} , which is comparable to the previous observations over the snowpack in Fairbanks, AK (0.12 – 1.06 cm s^{-1}).^{20,30} The variation of the modeled N_2O_5 deposition velocity in this work is driven by the N_2O_5 reactivity on the surface snowpack, as well as by the boundary layer stability. During Period I, the snowpack serves as a ClNO_2 source because of the high snow ClNO_2 yield (0.96, Figure 4) when the ambient temperature was low ($\sim 258 \text{ K}$, Figure 4). In Period I, 75% of the ClNO_2 produced in the snowpack undergoes hydrolysis, and only 25% is emitted out of the snowpack, leading to an upward net flux of $9 \pm 5 \times 10^8$ molecules $\text{cm}^{-2} \text{ s}^{-1}$ (average \pm standard deviation) of ClNO_2 into the near-surface atmosphere. ClNO_2 hydrolysis and its impact on the fate of snowpack ClNO_2 are discussed in Section 2.3. ClNO_2 production on atmospheric particles (within the NBL) is a factor of ~ 3 higher than that from the snowpack during Period I. During Period II, the ambient temperature was higher ($\sim 272 \text{ K}$), and hence the snowpack ClNO_2 yield reduced to 0.56 (Figure 4). In this case, with a higher f_{brine} , 99% of the ClNO_2 produced in the snowpack undergoes hydrolysis in the snowpack. Still, the model predicts a weak upward net flux of ClNO_2 during this period [$(4 \pm 5) \times 10^7$ molecules $\text{cm}^{-2} \text{ s}^{-1}$]. During Period III, however, the ambient air temperature increased above freezing ($> 273 \text{ K}$), which in

turn, decreased the modeled snowpack ClNO_2 yield to 0.05. Further, 100% of the snow-produced ClNO_2 undergoes hydrolysis within the snowpack, leading to a downward flux of $(4.1 \pm 0.3) \times 10^7$ molecules $\text{cm}^{-2} \text{ s}^{-1}$.

In summary, our modeling analysis demonstrates that under all of the temperature conditions tested, N_2O_5 reactions on the snowpack are a strong sink for N_2O_5 , consistent with previous studies.^{20,61} In the NBL, ClNO_2 production from particles is predicted to be the dominant pathway at 68–100%. The snowpack can be a net source or sink for ClNO_2 , depending on the snow grain brine volume fraction, which is controlled by temperature and salt content. In this way, the snowpack influences urban air quality.

2.3. ClNO_2 Hydrolysis. Whether the snow is a source or sink for ClNO_2 (Section 2.2) is largely controlled by the hydrolysis of ClNO_2 within the snowpack. In this section, the effect of snowpack ClNO_2 hydrolysis on its fate is examined using the model, with the hydrolysis rate derived from previous laboratory experiments.³² Using the same resistance analogue employed in the snowpack model (eq 3), the reactive uptake coefficient of ClNO_2 (γ_{ClNO_2}) on the NaCl solution from Behnke et al.³² can be translated into a pseudo-first-order ClNO_2 hydrolysis rate ($k_{\text{ClNO}_2-\text{H}_2\text{O}} \text{ s}^{-1}$), which ranges from 92 s^{-1} (in pure water) to 0.3 s^{-1} ($[\text{Cl}^-] = 4.7 \text{ M}$). Similar to γ_{ClNO_2} , $k_{\text{ClNO}_2-\text{H}_2\text{O}}$ also decreases with increasing chloride concentration, and the chloride concentration dependency appears to be nonlinear.³² As previously discussed, the estimated snow chloride concentration in the brine phase (calculated from bulk snow chloride and f_{brine}) for the 18 February 2016 case day was $\sim 2.3 \text{ M}$ (shown as the vertical dashed line in Figure S6). This corresponds to a $k_{\text{ClNO}_2-\text{H}_2\text{O}}$ of $\sim 2 \text{ s}^{-1}$. This constant ClNO_2 hydrolysis rate was then used in the model, with corrections for kinetic limitations (e.g., gas-diffusion, interfacial transport, bulk diffusion, see Section S4). The model-predicted downward ClNO_2 flux during Period III (Figure 4) is a result of rapid ClNO_2 hydrolysis in the snowpack.

The parameters governing the modeled snowpack ClNO_2 hydrolysis in this work remain uncertain, due in part to the lack of ClNO_2 hydrolysis studies at low temperatures. To the best of our knowledge, there are no published ClNO_2 uptake experiments on NaCl -containing aerosols or solutions for temperatures below 274 K that are relevant to wintertime conditions, including in high-latitude regions. The results from Fickert et al.⁷⁶ and Frenzel et al.⁷⁷ that reported up to 46% lower ClNO_2 uptake on pure water films when temperatures decreased from 287 to 274 K (Figure S6) demonstrate the importance of refining the parameterization of ClNO_2 hydrolysis in chloride-containing solutions. Therefore, it remains unclear how temperature may affect ClNO_2 hydrolysis on the natural snowpack, and thus, the hydrolysis rate used in the model ($k_{\text{ClNO}_2-\text{H}_2\text{O}} = 2 \text{ s}^{-1}$) is likely an upper limit.

3. CONCLUSIONS

This modeling study suggests that ClNO_2 may be produced from the snowpack, providing another source of ClNO_2 beyond atmospheric particles. Under cold conditions (e.g., $< 260 \text{ K}$), the saline snowpack is predicted to be a net source of ClNO_2 . However, a warmer snowpack (at near freezing temperatures) may facilitate ClNO_2 hydrolysis and serve as a net sink of ClNO_2 , consistent with a previous study in which

the authors found the ocean is a net sink of ClNO_2 .^{33,78} The results of this modeling study motivates the need to investigate the air–snow interactions controlling the production and removal of ClNO_2 . For example, the N_2O_5 reactive uptake coefficient and ClNO_2 yield on natural or artificial snow, as well as the ClNO_2 uptake on chloride-doped ice or artificial snow at a range of wintertime temperatures (e.g., 250–273 K) should be measured. We suggest that ClNO_2 hydrolysis (as inferred from limited laboratory experiments³²) may largely determine the fate of snow-produced ClNO_2 , and therefore, future studies should examine ClNO_2 hydrolysis on snow–ice. Investigation into the impacts of temperature, acidity, and chemical composition on the ClNO_2 multiphase chemistry will also provide valuable insights into the fate of ClNO_2 in snow. Last, but not least, direct flux observations of N_2O_5 and ClNO_2 above the snowpack will be useful to test predicted snowpack ClNO_2 production/removal.

To the best of our knowledge, this is the first study to examine the potential for ClNO_2 production from the snowpack, which may have broad implications in urban and suburban areas, where chloride-containing road salts are widely used as de-icing agents in winter.^{9,79} Snowpack ClNO_2 production was previously hypothesized to occur in the Arctic as well, where elevated N_2O_5 and ClNO_2 have been recently reported.³¹ This model of N_2O_5 uptake and ClNO_2 production in the snowpack is subject to potential uncertainties, such as the lack of vertically resolved meteorological measurements in quantifying the eddy diffusivity in an urban winter environment, as well as the poorly understood snowpack microphysics and chemistry. Another limitation of our modeling exercise is the lack of snowpack temperature measurements, with ambient air temperature used as a surrogate instead. Measurements of snow temperature, specific surface area, and density would provide additional insights and key constraints to the multiphase chemistry of N_2O_5 and ClNO_2 . In addition, because previous studies have shown reduced N_2O_5 uptake on organic-coated ambient particles,^{60,69–71} the role of surface snowpack organics on the uptake of N_2O_5 on snow and subsequent ClNO_2 chemistry remains unknown and warrants investigation.

■ ASSOCIATED CONTENT

SI Supporting Information

The Supporting Information is available free of charge at <https://pubs.acs.org/doi/10.1021/acsearthspacechem.0c00116>.

Schematic diagram of the 1-D multiphase photochemical model; vertical profiles of virtual potential temperature, wind speed, and calculated eddy diffusivity (K); calculated eddy diffusivity as a function of height and time for the case study; AIM-IC measured $\text{PM}_{2.5}$ chloride and nitrate concentrations and calculated $\gamma_{\text{N}_2\text{O}_5}$ ClNO_2 yield for particles; simulated vertical distributions; and ClNO_2 uptake coefficients for aqueous NaCl solutions at 291 K and various temperatures for pure water ([PDF](#))

■ AUTHOR INFORMATION

Corresponding Author

Kerri A. Pratt – Department of Chemistry and Department of Earth and Environmental Sciences, University of Michigan, Ann Arbor, Michigan 48109, United States;  orcid.org/0000-0002-1000-0004

0003-4707-2290; Phone: (734) 763-2871; Email: prattka@umich.edu

Authors

Siyuan Wang — Department of Chemistry, University of Michigan, Ann Arbor, Michigan 48109, United States

Stephen M. McNamara — Department of Chemistry, University of Michigan, Ann Arbor, Michigan 48109, United States

Katheryn R. Kolesar — Department of Chemistry, University of Michigan, Ann Arbor, Michigan 48109, United States

Nathaniel W. May — Department of Chemistry, University of Michigan, Ann Arbor, Michigan 48109, United States

Jose D. Fuentes — Department of Meteorology and Atmospheric Science, The Pennsylvania State University, University Park, Pennsylvania 16802, United States

Ryan D. Cook — Department of Chemistry, University of Michigan, Ann Arbor, Michigan 48109, United States

Matthew J. Gunsch — Department of Chemistry, University of Michigan, Ann Arbor, Michigan 48109, United States

Claire N. Mattson — Department of Chemistry, University of Michigan, Ann Arbor, Michigan 48109, United States

Rebecca S. Hornbrook — Atmospheric Chemistry Observations and Modeling Laboratory, National Center for Atmospheric Research, Boulder, Colorado 80301, United States

Eric C. Apel — Atmospheric Chemistry Observations and Modeling Laboratory, National Center for Atmospheric Research, Boulder, Colorado 80301, United States

Complete contact information is available at:

<https://pubs.acs.org/10.1021/acsearthspacechem.0c00116>

Notes

The authors declare no competing financial interest.

ACKNOWLEDGMENTS

Funding was provided by the University of Michigan and the National Science Foundation Atmospheric Chemistry program (AGS-1738588). K.R.K. was partially funded by a Dow Postdoctoral Fellowship in Sustainability from the University of Michigan. S.M.M. and N.W.M. were partially funded by U.S. Department of Education Graduate Assistance in Areas of National Need (GAANN) fellowships. The authors thank David J. Tanner and L. Gregory Huey (Georgia Institute of Technology) for providing the NO analyzer, Thomas B. Ryerson and Chelsea R. Thompson (NOAA) for providing the photolytic NO₂ converter, Alicia Kevelin, Madeline Parks, and Maria Morales (University of Michigan) for snow sampling and IC analysis, and Chelsea R. Thompson (NOAA) for assistance with NO_x measurements and helpful discussions. The National Center for Atmospheric Research is sponsored by the National Science Foundation; any opinions, findings, and conclusions or recommendations expressed in this publication are those of the authors and do not necessarily reflect the views of the National Science Foundation. The authors thank the reviewers for their comments that improved the manuscript and the editor for expeditiously handling the manuscript, especially given the current global challenges.

REFERENCES

(1) Osthoff, H. D.; Roberts, J. M.; Ravishankara, A. R.; Williams, E. J.; Lerner, B. M.; Sommariva, R.; Bates, T. S.; Coffman, D.; Quinn, P. K.; Dibb, J. E.; Stark, H.; Burkholder, J. B.; Talukdar, R. K.; Meagher, J.; Fehsenfeld, F. C.; Brown, S. S. High Levels of Nitryl Chloride in the Polluted Subtropical Marine Boundary Layer. *Nat. Geosci.* **2008**, *1*, 324–328.

(2) Thornton, J. A.; Kercher, J. P.; Riedel, T. P.; Wagner, N. L.; Cozic, J.; Holloway, J. S.; Dubé, W. P.; Wolfe, G. M.; Quinn, P. K.; Middlebrook, A. M.; Alexander, B.; Brown, S. S. A Large Atomic Chlorine Source Inferred from Mid-Continental Reactive Nitrogen Chemistry. *Nature* **2010**, *464*, 271–274.

(3) Simpson, W. R.; Brown, S. S.; Saiz-Lopez, A.; Thornton, J. A.; von Glasow, R. Tropospheric Halogen Chemistry: Sources, Cycling, and Impacts. *Chem. Rev.* **2015**, *115*, 4035–4062.

(4) Sarwar, G.; Simon, H.; Bhave, P.; Yarwood, G. Examining the Impact of Heterogeneous Nitryl Chloride Production on Air Quality across the United States. *Atmos. Chem. Phys.* **2012**, *12*, 6455–6473.

(5) Sarwar, G.; Simon, H.; Xing, J.; Mathur, R. Importance of Tropospheric ClNO₂ Chemistry across the Northern Hemisphere. *Geophys. Res. Lett.* **2014**, *41*, 4050–4058.

(6) Finlayson-Pitts, B. J.; Ezell, M. J.; Pitts, J. N. Formation of Chemically Active Chlorine Compounds by Reactions of Atmospheric NaCl Particles with Gaseous N₂O₅ and ClONO₂. *Nature* **1989**, *337*, 241–244.

(7) Mielke, L. H.; Furgeson, A.; Odame-Ankrah, C. A.; Osthoff, H. D. Ubiquity of ClNO₂ in the Urban Boundary Layer of Calgary, Alberta, Canada. *Can. J. Chem.* **2016**, *94*, 414–423.

(8) Burkholder, J. B.; Sander, S. P.; Abbott, J.; Barker, J. R.; Huie, R. E.; Kolb, C. E.; Kurylo, M. J.; Orkin, V. L.; Wilmouth, D. M.; Wine, P. H. *Chemical Kinetics and Photochemical Data for Use in Atmospheric Studies, Evaluation No. 18; JPL Publication 10-6*; Jet Propulsion Laboratory: Pasadena, 2015; <http://jpldataeval.jpl.nasa.gov>.

(9) Kolesar, K. R.; Mattson, C. N.; Peterson, P. K.; May, N. W.; Prendergast, R. K.; Pratt, K. A. Increases in Wintertime PM_{2.5} Sodium and Chloride Linked to Snowfall and Road Salt Application. *Atmos. Environ.* **2018**, *177*, 195–202.

(10) George, C.; Ponche, J. L.; Mirabel, P.; Behnke, W.; Scheer, V.; Zetzsch, C. Study of the Uptake of N₂O₅ by Water and NaCl Solutions. *J. Phys. Chem.* **1994**, *98*, 8780–8784.

(11) Lopez-Hilfiker, F. D.; Constantin, K.; Kercher, J. P.; Thornton, J. A. Temperature Dependent Halogen Activation by N₂O₅ Reactions on Halide-Doped Ice Surfaces. *Atmos. Chem. Phys.* **2012**, *12*, 5237–5247.

(12) Lazarcik, J.; Dibb, J. Evidence of Road Salt in New Hampshire's Snowpack Hundreds of Meters from Roadways. *Geosciences* **2017**, *7*, 54–61.

(13) Grannas, A. M.; Jones, A. E.; Dibb, J.; Ammann, M.; Anastasio, C.; Beine, H. J.; Bergin, M.; Bottenheim, J.; Boxe, C. S.; Carver, G.; Chen, G.; Crawford, J. H.; Dominé, F.; Frey, M. M.; Guzmán, M. I.; Heard, D. E.; Helmig, D.; Hoffmann, M. R.; Honrath, R. E.; Huey, L. G.; Hutterli, M.; Jacobi, H. W.; Klán, P.; Lefer, B.; McConnell, J.; Plane, J.; Sander, R.; Savarino, J.; Shepson, P. B.; Simpson, W. R.; Sodeau, J. R.; von Glasow, R.; Weller, R.; Wolff, E. W.; Zhu, T. An Overview of Snow Photochemistry: Evidence, Mechanisms and Impacts. *Atmos. Chem. Phys.* **2007**, *7*, 4329–4373.

(14) Albert, M. R.; Grannas, A. M.; Bottenheim, J.; Shepson, P. B.; Perron, F. E. Processes and Properties of Snow–Air Transfer in the High Arctic with Application to Interstitial Ozone at Alert, Canada. *Atmos. Environ.* **2002**, *36*, 2779–2787.

(15) Domine, F.; Albert, M.; Huthwelker, T.; Jacobi, H.-W.; Kokhanovsky, A. A.; Lehning, M.; Picard, G.; Simpson, W. R. Snow Physics as Relevant to Snow Photochemistry. *Atmos. Chem. Phys.* **2008**, *8*, 171–208.

(16) Domine, F.; Shepson, P. B. Air–Snow Interactions and Atmospheric Chemistry. *Science* **2002**, *297*, 1506–1510.

(17) Chen, Q.; Edebeli, J.; McNamara, S. M.; Kulju, K. D.; May, N. W.; Bertman, S. B.; Thanekar, S.; Fuentes, J. D.; Pratt, K. A. HONO, Particulate Nitrite, and Snow Nitrite at a Midlatitude Urban Site during Wintertime. *ACS Earth Space Chem.* **2019**, *3*, 811–822.

(18) Honrath, R. E.; Peterson, M. C.; Dziobak, M. P.; Dibb, J. E.; Arsenault, M. A.; Green, S. A. Release of NO_x from Sunlight-Irradiated Midlatitude Snow. *Geophys. Res. Lett.* **2000**, *27*, 2237–2240.

(19) Zatko, M. C.; Grenfell, T. C.; Alexander, B.; Doherty, S. J.; Thomas, J. L.; Yang, X. The Influence of Snow Grain Size and Impurities on the Vertical Profiles of Actinic Flux and Associated NO_x Emissions on the Antarctic and Greenland Ice Sheets. *Atmos. Chem. Phys.* **2013**, *13*, 3547–3567.

(20) Joyce, P. L.; von Glasow, R.; Simpson, W. R. The Fate of NO_x Emissions Due to Nocturnal Oxidation at High Latitudes: 1-D Simulations and Sensitivity Experiments. *Atmos. Chem. Phys.* **2014**, *14*, 7601–7616.

(21) Honrath, R. E.; Jaffe, D. A. The Seasonal Cycle of Nitrogen Oxides in the Arctic Troposphere at Barrow, Alaska. *J. Geophys. Res.: Atmos.* **1992**, *97*, 20615–20630.

(22) Honrath, R. E.; Lu, Y.; Peterson, M. C.; Dibb, J. E.; Arsenault, M. A.; Cullen, N. J.; Steffen, K. Vertical Fluxes of NO_x, HONO, and HNO₃ above the Snowpack at Summit, Greenland. *Atmos. Environ.* **2002**, *36*, 2629–2640.

(23) Honrath, R. E.; Peterson, M. C.; Guo, S.; Dibb, J. E.; Shepson, P. B.; Campbell, B. Evidence of NO_x Production within or upon Ice Particles in the Greenland Snowpack. *Geophys. Res. Lett.* **1999**, *26*, 695–698.

(24) Barret, M.; Domine, F.; Houdier, S.; Gallet, J.-C.; Weibring, P.; Walega, J.; Fried, A.; Richter, D. Formaldehyde in the Alaskan Arctic Snowpack: Partitioning and Physical Processes Involved in Air-Snow Exchanges. *J. Geophys. Res.: Atmos.* **2011**, *116*, D00R03.

(25) Custard, K. D.; Raso, A. R. W.; Shepson, P. B.; Staebler, R. M.; Pratt, K. A. Production and Release of Molecular Bromine and Chlorine from the Arctic Coastal Snowpack. *ACS Earth Space Chem.* **2017**, *1*, 142–151.

(26) Pratt, K. A.; Custard, K. D.; Shepson, P. B.; Douglas, T. A.; Pöhler, D.; General, S.; Zielcke, J.; Simpson, W. R.; Platt, U.; Tanner, D. J.; Gregory Huey, L.; Carlsen, M.; Stirm, B. H. Photochemical Production of Molecular Bromine in Arctic Surface Snowpacks. *Nat. Geosci.* **2013**, *6*, 351–356. <http://www.nature.com/ngeo/journal/v6/n5/abs/ngeo1779.html#supplementary-information>

(27) Raso, A. R. W.; Custard, K. D.; May, N. W.; Tanner, D.; Newburn, M. K.; Walker, L.; Moore, R. J.; Huey, L. G.; Alexander, L.; Shepson, P. B.; Pratt, K. A. Active Molecular Iodine Photochemistry in the Arctic. *Proc. Natl. Acad. Sci.* **2017**, *114*, 10053–10058.

(28) Helmig, D.; Boylan, P.; Johnson, B.; Oltmans, S.; Fairall, C.; Staebler, R.; Weinheimer, A.; Orlando, J.; Knapp, D. J.; Montzka, D. D.; Flocke, F.; Fries, U.; Sihler, H.; Shepson, P. B. Ozone Dynamics and Snow-Atmosphere Exchanges during Ozone Depletion Events at Barrow, Alaska. *J. Geophys. Res.: Atmos.* **2012**, *117*, 1–15.

(29) Edwards, P. M.; Young, C. J.; Aikin, K.; DeGouw, J.; Dubé, W. P.; Geiger, F.; Gilman, J.; Helmig, D.; Holloway, J. S.; Kercher, J.; Lerner, B.; Martin, R.; McLaren, R.; Parrish, D. D.; Peischl, J.; Roberts, J. M.; Ryerson, T. B.; Thornton, J.; Warneke, C.; Williams, E. J.; Brown, S. S. Ozone Photochemistry in an Oil and Natural Gas Extraction Region during Winter: Simulations of a Snow-Free Season in the Uintah Basin, Utah. *Atmos. Chem. Phys.* **2013**, *13*, 8955–8971.

(30) Huff, D. M.; Joyce, P. L.; Fochesatto, G. J.; Simpson, W. R. Deposition of Dinitrogen Pentoxide, N₂O₅ to the Snowpack at High Latitudes. *Atmos. Chem. Phys.* **2011**, *11*, 4929–4938.

(31) McNamara, S. M.; Raso, A. R. W.; Wang, S.; Thanekar, S.; Boone, E. J.; Kolesar, K. R.; Peterson, P. K.; Simpson, W. R.; Fuentes, J. D.; Shepson, P. B.; Pratt, K. A. Springtime Nitrogen Oxide-Influenced Chlorine Chemistry in the Coastal Arctic. *Environ. Sci. Technol.* **2019**, *53*, 8057–8067.

(32) Behnke, W.; George, C.; Scheer, V.; Zetzsch, C. Production and Decay of ClNO₂ from the Reaction of Gaseous N₂O₅ with NaCl Solution: Bulk and Aerosol Experiments. *J. Geophys. Res.: Atmos.* **1997**, *102*, 3795–3804.

(33) Kim, M. J.; Farmer, D. K.; Bertram, T. H. A Controlling Role for the Air-sea Interface in the Chemical Processing of Reactive Nitrogen in the Coastal Marine Boundary Layer. *Proc. Natl. Acad. Sci.* **2014**, *111*, 3943–3948.

(34) Thomas, J. L.; Stutz, J.; Lefer, B.; Huey, L. G.; Toyota, K.; Dibb, J. E.; von Glasow, R. Modeling Chemistry in and above Snow at Summit, Greenland – Part 1: Model Description and Results. *Atmos. Chem. Phys.* **2011**, *11*, 4899–4914.

(35) Thomas, J. L.; Dibb, J. E.; Huey, L. G.; Liao, J.; Tanner, D.; Lefer, B.; von Glasow, R.; Stutz, J. Modeling Chemistry in and above Snow at Summit, Greenland – Part 2: Impact of Snowpack Chemistry on the Oxidation Capacity of the Boundary Layer. *Atmos. Chem. Phys.* **2012**, *12*, 6537–6554.

(36) Toyota, K.; McConnell, J. C.; Staebler, R. M.; Dastoor, A. P. Air–Snowpack Exchange of Bromine, Ozone and Mercury in the Springtime Arctic Simulated by the 1-D Model PHANTAS - Part 1: In-Snow Bromine Activation and Its Impact on Ozone. *Atmos. Chem. Phys.* **2014**, *14*, 4101–4133.

(37) Toyota, K.; Dastoor, A. P.; Ryzhkov, A. Air–Snowpack Exchange of Bromine, Ozone and Mercury in the Springtime Arctic Simulated by the 1-D Model PHANTAS - Part 2: Mercury and Its Speciation. *Atmos. Chem. Phys.* **2014**, *14*, 4135–4167.

(38) Chan, H. G.; Frey, M. M.; King, M. D. Modelling the Physical Multiphase Interactions of HNO₃ between Snow and Air on the Antarctic Plateau (Dome C) and Coast (Halley). *Atmos. Chem. Phys.* **2018**, *18*, 1507–1534.

(39) Song, S.; Angot, H.; Selin, N. E.; Gallée, H.; Sprovieri, F.; Pirrone, N.; Helmig, D.; Savarino, J.; Magand, O.; Dommergue, A. Understanding Mercury Oxidation and Air–Snow Exchange on the East Antarctic Plateau: A Modeling Study. *Atmos. Chem. Phys.* **2018**, *18*, 15825–15840.

(40) McNamara, S. M.; Kolesar, K. R.; Wang, S.; Kirpes, R. M.; May, N. W.; Gunsch, M. J.; Cook, R. D.; Fuentes, J. D.; Hornbrook, R. S.; Apel, E. C.; China, S.; Laskin, A.; Pratt, K. A. Observation of Road Salt Aerosol Driving Inland Wintertime Atmospheric Chlorine Chemistry. *ACS Cent. Sci.* **2020**, *6*, 684–694.

(41) Wang, S.; Pratt, K. A. Molecular Halogens Above the Arctic Snowpack: Emissions, Diurnal Variations, and Recycling Mechanisms. *J. Geophys. Res.: Atmos.* **2017**, *122*, 11991–12007.

(42) Liao, J.; Sihler, H.; Huey, L. G.; Neuman, J. A.; Tanner, D. J.; Friess, U.; Platt, U.; Flocke, F. M.; Orlando, J. J.; Shepson, P. B. A Comparison of Arctic BrO Measurements by Chemical Ionization Mass Spectrometry and Long Path-differential Optical Absorption Spectroscopy. *J. Geophys. Res.: Atmos.* **2011**, *116*, D00R02.

(43) Sjostedt, S. J.; Huey, L. G.; Tanner, D. J.; Peischl, J.; Chen, G.; Dibb, J. E.; Lefer, B.; Hutterli, M. A.; Beyersdorf, A. J.; Blake, N. J.; Blake, D. R.; Sueper, D.; Ryerson, T.; Burkhardt, J.; Stohl, A. Observations of Hydroxyl and the Sum of Peroxy Radicals at Summit, Greenland during Summer 2003. *Atmos. Environ.* **2007**, *41*, 5122–5137.

(44) Markovic, M. Z.; VandenBoer, T. C.; Murphy, J. G. Characterization and Optimization of an Online System for the Simultaneous Measurement of Atmospheric Water-Soluble Constituents in the Gas and Particle Phases. *J. Environ. Monit.* **2012**, *14*, 1872–1884.

(45) Apel, E. C.; Hills, A. J.; Leub, R.; Zindel, S.; Eisele, S.; Riemer, D. D. A Fast-GC/MS System to Measure C₂ to C₄ Carbonyls and Methanol Aboard Aircraft. *J. Geophys. Res.* **2003**, *108*, 8794–8811.

(46) Apel, E. C.; Calvert, J. G.; Fehsenfeld, F. C. The Nonmethane Hydrocarbon Intercomparison Experiment (NOMHICE): Tasks 1 and 2. *J. Geophys. Res.: Atmos.* **1994**, *99*, 16651–16664.

(47) Apel, E. C.; Calvert, J. G.; Gilpin, T. M.; Fehsenfeld, F. C.; Parrish, D. D.; Lonneman, W. A. The Nonmethane Hydrocarbon Intercomparison Experiment (NOMHICE): Task 3. *J. Geophys. Res.: Atmos.* **1999**, *104*, 26069–26086.

(48) Michigan Air Quality: Real-time Data. <http://www.deqmiair.org/monitoringdata.cfm?site=1687&date=2%2F19%2F2016> (accessed Jun 28, 2019).

(49) Dlugokencky, E. J.; Lang, P. M.; Crotwell, A. M.; Masarie, K. A.; Crotwell, M. J.; Thoning, K. W. Atmospheric Methane Dry Air Mole Fractions from the NOAA ESRL Carbon Cycle Cooperative Global Air Sampling Network, 1983–2013, Version: 2014-06-24. [atfp.cdm.noaa.gov/data/trace_gases/ch4/flask/surface2013](http://cdm.noaa.gov/data/trace_gases/ch4/flask/surface2013).

(50) Chang, A. T. C.; Foster, J. L.; Hall, D. K.; Goodison, B. E.; Walker, A. E.; Metcalfe, J. R.; Harby, A. Snow Parameters Derived

from Microwave Measurements during the BOREAS Winter Field Campaign. *J. Geophys. Res.: Atmos.* **1997**, *102*, 29663–29671.

(51) Molotch, N. P.; Barnard, D. M.; Burns, S. P.; Painter, T. H. Measuring Spatiotemporal Variation in Snow Optical Grain Size under a Subalpine Forest Canopy Using Contact Spectroscopy. *Water Resour. Res.* **2016**, *52*, 7513–7522.

(52) Bartels-Rausch, T.; Jacobi, H.-W.; Kahan, T. F.; Thomas, J. L.; Thomson, E. S.; Abbatt, J. P. D.; Ammann, M.; Blackford, J. R.; Bluhm, H.; Boxe, C.; Domine, F.; Frey, M. M.; Gladich, I.; Guzmán, M. I.; Heger, D.; Huthwelker, T.; Klán, P.; Kuhs, W. F.; Kuo, M. H.; Maus, S.; Moussa, S. G.; McNeill, V. F.; Newberg, J. T.; Pettersson, J. B. C.; Roeselová, M.; Sodeau, J. R. A Review of Air–Ice Chemical and Physical Interactions (AICI): Liquids, Quasi-Liquids, and Solids in Snow. *Atmos. Chem. Phys.* **2014**, *14*, 1587–1633.

(53) Cho, H.; Shepson, P. B.; Barrie, L. A.; Cowin, J. P.; Zaveri, R. NMR Investigation of the Quasi-Brine Layer in Ice/Brine Mixtures. *J. Phys. Chem. B* **2002**, *106*, 11226–11232.

(54) Bertram, T. H.; Thornton, J. A. Toward a General Parameterization of N_2O_5 Reactivity on Aqueous Particles: The Competing Effects of Particle Liquid Water, Nitrate and Chloride. *Atmos. Chem. Phys.* **2009**, *9*, 8351–8363.

(55) Gaston, C. J.; Thornton, J. A. Reacto-Diffusive Length of N_2O_5 in Aqueous Sulfate- and Chloride-Containing Aerosol Particles. *J. Phys. Chem. A* **2016**, *120*, 1039–1045.

(56) Schweitzer, F.; Mirabel, P.; George, C. Multiphase Chemistry of N_2O_5 , ClNO_2 , and BrNO_2 . *J. Phys. Chem. A* **1998**, *102*, 3942–3952.

(57) Pöschl, U.; Rudich, Y.; Ammann, M. Kinetic Model Framework for Aerosol and Cloud Surface Chemistry and Gas-Particle Interactions – Part 1: General Equations, Parameters, and Terminology. *Atmospheric Chemistry and Physics* **2007**, *7*, 5989–6023.

(58) Sander, R. Compilation of Henry's Law Constants (Version 4.0) for Water as Solvent. *Atmos. Chem. Phys.* **2015**, *15*, 4399–4981.

(59) Stewart, D. J.; Griffiths, P. T.; Cox, R. A. Reactive Uptake Coefficients for Heterogeneous Reaction of N_2O_5 with Submicron Aerosols of NaCl and Natural Sea Salt. *Atmos. Chem. Phys.* **2004**, *4*, 1381–1388.

(60) Thornton, J. A.; Abbatt, J. P. D. N_2O_5 Reaction on Submicron Sea Salt Aerosol: Kinetics, Products, and the Effect of Surface Active Organics. *J. Phys. Chem. A* **2005**, *109*, 10004–10012.

(61) Geyer, A.; Stutz, J. Vertical Profiles of NO_3 , N_2O_5 , O_3 , and NO_x in the Nocturnal Boundary Layer: 2. Model Studies on the Altitude Dependence of Composition and Chemistry. *J. Geophys. Res.: Atmos.* **2004**, *109*, D12307.

(62) Kravsek, L.; Simpson, W. R.; Carlson, D.; Domine, F.; Douglas, T. A.; Sturm, M. The Chemical Composition of Surface Snow in the Arctic: Examining Marine, Terrestrial, and Atmospheric Influences. *Atmos. Environ.* **2012**, *50*, 349–359.

(63) Bertram, T. H.; Thornton, J. A.; Riedel, T. P.; Middlebrook, A. M.; Bahreini, R.; Bates, T. S.; Quinn, P. K.; Coffman, D. J. Direct Observations of N_2O_5 Reactivity on Ambient Aerosol Particles. *Geophys. Res. Lett.* **2009**, *36*, L19803.

(64) McDuffie, E. E.; Fibiger, D. L.; Dubé, W. P.; Hilfiker, F. L.; Lee, B. H.; Jaeglé, L.; Guo, H.; Weber, R. J.; Reeves, J. M.; Weinheimer, A. J.; Schroder, J. C.; Campuzano-Jost, P.; Jimenez, J. L.; Dibb, J. E.; Veres, P.; Ebbin, C.; Sparks, T. L.; Wooldridge, P. J.; Cohen, R. C.; Campos, T.; Hall, S. R.; Ullmann, K.; Roberts, J. M.; Thornton, J. A.; Brown, S. S. ClNO_2 Yields From Aircraft Measurements During the 2015 WINTER Campaign and Critical Evaluation of the Current Parameterization. *J. Geophys. Res.: Atmos.* **2018**, *123*, 12994–13015.

(65) Phillips, G. J.; Tang, M. J.; Thieser, J.; Brickwedde, B.; Schuster, G.; Bohn, B.; Lelieveld, J.; Crowley, J. N. Significant Concentrations of Nitryl Chloride Observed in Rural Continental Europe Associated with the Influence of Sea Salt Chloride and Anthropogenic Emissions. *Geophys. Res. Lett.* **2012**, *39*, L10811.

(66) Riedel, T. P.; Bertram, T. H.; Crisp, T. A.; Williams, E. J.; Lerner, B. M.; Vlasenko, A.; Li, S.-M.; Gilman, J.; de Gouw, J.; Bon, D. M.; Wagner, N. L.; Brown, S. S.; Thornton, J. A. Nitryl Chloride and Molecular Chlorine in the Coastal Marine Boundary Layer. *Environ. Sci. Technol.* **2012**, *46*, 10463–10470.

(67) Tham, Y. J.; Wang, Z.; Li, Q.; Wang, W.; Wang, X.; Lu, K.; Ma, N.; Yan, C.; Kecorius, S.; Wiedensohler, A.; Zhang, Y.; Wang, T. Heterogeneous N_2O_5 Uptake Coefficient and Production Yield of ClNO_2 in Polluted Northern China: Roles of Aerosol Water Content and Chemical Composition. *Atmos. Chem. Phys.* **2018**, *18*, 13155–13171.

(68) Mielke, L. H.; Stutz, J.; Tsai, C.; Hurlock, S. C.; Roberts, J. M.; Veres, P. R.; Froyd, K. D.; Hayes, P. L.; Cubison, M. J.; Jimenez, J. L.; Washenfelder, R. A.; Young, C. J.; Gilman, J. B.; de Gouw, J. A.; Flynn, J. H.; Grossberg, N.; Lefer, B. L.; Liu, J.; Weber, R. J.; Osthoff, H. D. Heterogeneous Formation of Nitryl Chloride and Its Role as a Nocturnal NO_x Reservoir Species during CalNex-LA 2010. *J. Geophys. Res.: Atmos.* **2013**, *118*, 10638–10652.

(69) Anttila, T.; Kiendler-Scharr, A.; Tillmann, R.; Mentel, T. F. On the Reactive Uptake of Gaseous Compounds by Organic-Coated Aqueous Aerosols: Theoretical Analysis and Application to the Heterogeneous Hydrolysis of N_2O_5 . *J. Phys. Chem. A* **2006**, *110*, 10435–10443.

(70) Gaston, C. J.; Thornton, J. A.; Ng, N. L. Reactive Uptake of N_2O_5 to Internally Mixed Inorganic and Organic Particles: The Role of Organic Carbon Oxidation State and Inferred Organic Phase Separations. *Atmos. Chem. Phys.* **2014**, *14*, 5693–5707.

(71) Ryder, O. S.; Campbell, N. R.; Morris, H.; Forestieri, S.; Ruppel, M. J.; Cappa, C.; Tivanski, A.; Prather, K.; Bertram, T. H. Role of Organic Coatings in Regulating N_2O_5 Reactive Uptake to Sea Spray Aerosol. *J. Phys. Chem. A* **2015**, *119*, 11683–11692.

(72) Staudt, S.; Gord, J. R.; Karimova, N. V.; McDuffie, E. E.; Brown, S. S.; Gerber, R. B.; Nathanson, G. M.; Bertram, T. H. Sulfate and Carboxylate Suppress the Formation of ClNO_2 at Atmospheric Interfaces. *ACS Earth Space Chem.* **2019**, *3*, 1987–1997.

(73) Ryder, O. S.; Ault, A. P.; Cahill, J. F.; Guasco, T. L.; Riedel, T. P.; Cuadra-Rodriguez, L. A.; Gaston, C. J.; Fitzgerald, E.; Lee, C.; Prather, K. A.; Bertram, T. H. On the Role of Particle Inorganic Mixing State in the Reactive Uptake of N_2O_5 to Ambient Aerosol Particles. *Environ. Sci. Technol.* **2014**, *48*, 1618–1627.

(74) Young, C. J.; Washenfelder, R. A.; Roberts, J. M.; Mielke, L. H.; Osthoff, H. D.; Tsai, C.; Pikelnaya, O.; Stutz, J.; Veres, P. R.; Cochran, A. K.; VandenBoer, T. C.; Flynn, J.; Grossberg, N.; Haman, C. L.; Lefer, B.; Stark, H.; Graus, M.; de Gouw, J.; Gilman, J. B.; Kuster, W. C.; Brown, S. S. Vertically Resolved Measurements of Nighttime Radical Reservoirs in Los Angeles and Their Contribution to the Urban Radical Budget. *Environ. Sci. Technol.* **2012**, *46*, 10965–10973.

(75) Wang, T.; Tham, Y. J.; Xue, L.; Li, Q.; Zha, Q.; Wang, Z.; Poon, S. C. N.; Dubé, W. P.; Blake, D. R.; Louie, P. K. K.; Luk, C. W. Y.; Tsui, W.; Brown, S. S. Observations of Nitryl Chloride and Modeling Its Source and Effect on Ozone in the Planetary Boundary Layer of Southern China. *J. Geophys. Res.: Atmos.* **2016**, *121*, 2476–2489.

(76) Fickert, S.; Helleis, F.; Adams, J. W.; Moortgat, G. K.; Crowley, J. N. Reactive Uptake of ClNO_2 on Aqueous Bromide Solutions. *J. Phys. Chem. A* **1998**, *102*, 10689–10696.

(77) Frenzel, A.; Scheer, V.; Sikorski, R.; George, C.; Behnke, W.; Zetsch, C. Heterogeneous Interconversion Reactions of BrNO_2 , ClNO_2 , Br_2 , and Cl_2 . *J. Phys. Chem. A* **1998**, *102*, 1329–1337.

(78) McCaslin, L. M.; Johnson, M. A.; Gerber, R. B. Mechanisms and Competition of Halide Substitution and Hydrolysis in Reactions of N_2O_5 with Seawater. *Sci. Adv.* **2019**, *5*, No. eaav6503.

(79) Ramakrishna, D. M.; Viraraghavan, T. Environmental Impact of Chemical Deicers – A Review. *Water, Air, Soil Pollut.* **2005**, *166*, 49–63.